Clinical Biomechanics 50 (2017) 122–129

Contents lists available at ScienceDirect

Clinical Biomechanics

journal homepage: www.elsevier.com/locate/clinbiomech

Numerical evaluation of bone remodelling and adaptation considering different hip prosthesis designs

Ievgen Levadnyi[a], Jan Awrejcewicz[a,b,*], José Eduardo Gubaua[c], Jucélio Tomás Pereira[c]

[a] Lodz University of Technology, Department of Automation, Biomechanics and Mechatronics, 1/15 Stefanowski Str., 90–924 Lodz, Poland
[b] Warsaw University of Technology, Institute of Vehicles, 84 Narbutta Str., 02–524 Warsaw, Poland
[c] Federal University of Paraná, Laboratory of Computational Solid Mechanics, Curitiba, Brazil

ARTICLE INFO

Keywords:
Bone remodelling
Proximal femur
Finite element
Hip replacement
Short stem
Resurfacing

ABSTRACT

Background: The change in mechanical properties of femoral cortical bone tissue surrounding the stem of the hip endoprosthesis is one of the causes of implant instability. We present an analysis used to determine the best conditions for long-term functioning of the bone–implant system, which will lead to improvement of treatment results.

Methods: In the present paper, a finite element method coupled with a bone remodelling model is used to evaluate how different three-dimensional prosthesis models influence distribution of the density of bone tissue. The remodelling process begins after the density field is obtained from a computed tomography scan. Then, an isotropic Stanford model is employed to solve the bone remodelling process and verify bone tissue adaptation in relation to different prosthesis models.

Findings: The study results show that the long-stem models tend not to transmit loads to proximal regions of bone, which causes the stress-shielding effect. Short stems or application in the calcar region provide a favourable environment for transfer of loads to the proximal region, which allows for maintenance of bone density and, in some cases, for a positive variation, which causes absence of the aseptic loosening of an implant. In the case of hip resurfacing, bone mineral density changes slightly and is closest to an intact femur.

Interpretation: Installation of an implant modifies density distribution and stress field in the bone. Thus, bone tissue is stimulated in a different way than before total hip replacement, which evidences Wolff's law, according to which bone tissue adapts itself to the loads imposed on it. The results suggest that potential stress shielding in the proximal femur and cortical hypertrophy in the distal femur may, in part, be reduced through the use of shorter stems, instead of long ones, provided stem fixation is adequate.

1. Introduction

Bone remodelling is a process of renovation of bone tissue, which replaces old and deteriorated bone with new and healthy tissue (Lemaire et al., 2004). This process takes place throughout the life of an individual. Not every tissue in a human body has the same ability to renew itself. For example, when the cartilages surrounding the bones that comprise a joint are not healthy, a process in which the destruction level is higher than the creation level takes place, causing osteoarthritis. With degradation of cartilage tissue, the bones of the joint start to be in contact with each other, which causes friction and pain. Such a condition reduces life quality of the individual, causing discomfort and pain in simple daily activities such as walking. To solve the above-mentioned problem in a hip joint, a surgical procedure called hip arthroplasty is implemented. This surgery aims at replacing a damaged joint with an artificial one, which allows for improvement of individual health (Ethgen et al., 2004; Froimson et al., 2007; Jenkins et al., 2013). According to the USA analytical services, the number of total hip endoprosthesis replacements will increase by 180% by 2030 (Kelly et al., 2009).

A successful solution to the issues related to the improvement of the structural strength of the prosthesis and the decrease in wear of the acetabular component has moved the area of interests of scientific research into the field of mechanics of the interaction between the implant and bone tissue. Despite the fact that this issue has been a topic of a large number of clinical observations, mechanical aspects of the problem remain understudied.

The loss of stable fixation of a hip endoprosthesis stem, which is a clinical reason for a hip revision, may have different causes (Engh Jr et al., 1999; Sumner, 2015). Often, in implanted femurs with long-stem

* Corresponding author at: Lodz University of Technology, Department of Automation, Biomechanics and Mechatronics, 1/15 Stefanowski St., 90-924 Lodz, Poland.
E-mail addresses: jan.awrejcewicz@p.lodz.pl, awrejcew@p.lodz.pl (J. Awrejcewicz).

http://dx.doi.org/10.1016/j.clinbiomech.2017.10.015
Received 12 August 2016; Accepted 17 October 2017

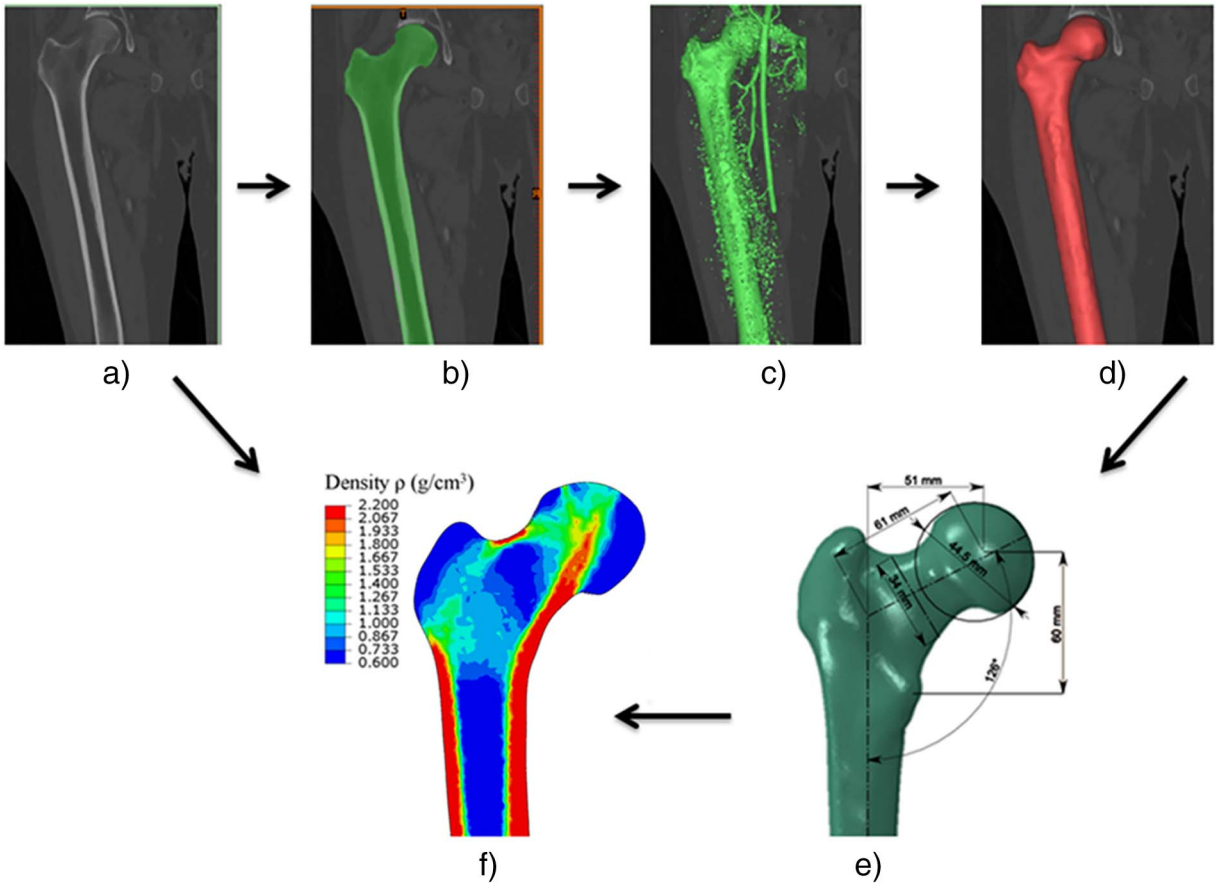

Fig. 1. Three-dimensional model of the femur created from CT images. The main stages of creating this 3D model are: (a) obtaining images of computed tomography of the femur; (b) loading the CT image and segmentation of the object; (c) forming the primary bone geometry; (d–e) smoothing the model and obtaining solid geometry of the bone; (f) assignment of the mechanical characteristics of the femur.

implants, the upper part of the femur receives fewer loads, leading to bone loss (proximal stress shielding), while bone around the distal end of the femoral component is overloaded and cortical hypertrophy may occur. The given changes in the femur are caused by redistribution of load on bone tissue under the endoprosthesis, and may be considered an adaptive reaction of a human organism to new functional conditions. The magnitudes of non-specific loads acting on the bone, which are generated after endoprosthesis implantation, are less than the breaking loads. That is why standard static failure criteria do not enable forecasting of the durability of the bone–implant system. The models of fatigue damage accumulation are also inapplicable for describing bone failure processes because of incessant replacement of an old substance with a new one, which proceeds in a living tissue. The models of bone tissue adaptive remodelling reflect the relationship between the bone mechanical properties and the load.

Currently, there are many designs of femoral stems, including straight, tapered, short length, and anatomical. Therefore, the study of the interaction between the stem endoprosthesis and femur, also taking into account adaptive properties of the bone, is important for medical practice problems.

For assistance of the development of not only prostheses, but also engineering projects in general, a Finite Element Method (FEM), which enables extensive studies to be conducted at reduced cost and in a short time, can be implemented. Thanks to the FEM, it is possible to avoid difficulties associated with the use of analytical methods for calculation of the stress–strain state of biomechanical systems and, most importantly, to obtain results with high accuracy (De Santis et al., 2000; Sabatini and Goswami, 2008; Yamako et al., 2014).

Many authors have conducted research related to the use of different prosthesis models evaluated using the FEM. Senalp et al. (2007) studied four varying curvatures of the stem of the hip prosthesis and evaluated static, dynamic and fatigue behaviour of these designs. Pal et al. (2010) studied load transfer and potential failure mechanisms of a short-stem femoral resurfacing component in the bone remodelling process. In the same line of research, Rothstock et al. (2011) investigated the influence of both different bone–implant interface conditions and the inner implant shape on bone strains. They compared the results with those obtained for the host bone as well as supplemented the study with an analysis of what happens in the consequent bone remodelling. Herrera et al. (2014) analysed the bone remodelling process associated with two cemented stem models randomly implanted in patients older than 75 years of age.

In this work, new numerical models for bone remodelling are not developed, but the relationship between two-year bone adaptation to mechanical loading and different endoprosthesis types are studied. Several objectives of this work can be listed, including, first of all, to make 3D FE models (one of a healthy femur and the other of a femur after stem implantation) from CT scans corresponding to the healthy femur. This enables correct positioning of the stem in the operated femur in order to study its mechanical performance (especially proper load transfer through contact between the bone and the prosthesis). The second objective was to analyse and check the results of changes in the bone mineral density (BMD) in every Gruen zone after implantation of different types of endoprosthesis, and to determine changes in the stress-strain state of implants. The last objective was to validate the obtained FE results by qualitative comparison with clinical trials.

Our working hypotheses are as follows: (i) short-stem implants would provide more physiological bone stress distribution as compared

to the long-stem implants; (ii) an additional collar for long-stem implants would reduce bone loosening in the proximal part of the femur; (iii) no significant difference in bone density change when resurfacing using.

2. Methods

2.1. Femur model

For the analysis, a three-dimensional model of the femur has been developed based on the results of computed tomography (CT), which allows creation of three-dimensional models of organs with high accuracy of the shape and properties of soft and bone tissues, giving almost an in vivo model. The algorithm of generation of a three-dimensional geometric model of the femur consisted of several steps (Fig. 1). For this study, five femurs were scanned from five male patients to obtain a set of slices by computed tomography. The CT scan images of the femurs did not present any abnormality or musculoskeletal impairment, and the subjects had no history of either neuromuscular or musculoskeletal disorders. The mean patient age was 65 years (SD ± 22 years). The patients were scanned at the Dnipropetrovsk State Medical Academy, using an AQUILION RXL 16 (Toshiba Medical Systems) 16-slice computed tomography scanner. DICOM images were obtained with a 0.5 mm slice thickness. Then, CT images of the femur were downloaded for subsequent segmentation of the object. The CT data were processed using MIMICS (Materialise, N.V. – Belgium) software. Segmentation of the images was performed based on the obtained axial projections of the object, using the selection field in a form of a separate mask. The next step comprised the creation of a three-dimensional object on the mask in STL format. Then, the quality of the three-dimensional object was improved by using different functions of surface smoothing.

The mechanical characteristics of the femur were found by calculating the analytical dependences between the Hounsfield units (HU) obtained from the analysis of computed tomograms (Fig. 1). Hounsfield units determine the dependence between the radiographic density of the femur tissue, presented in arbitrary units (Cann, 1988; Peng et al., 2007), and the actual bone density – ρ (g/cm^3). In our study, the CT machine was calibrated to acquire a relationship between HU and BMD using the handmade Calibration Phantom. The CT Calibration Phantom contains seven tubes with different (50, 200, 400, 600, 800, 1000, and 1200 mg/mL) concentrations of K2HPO4 in distilled water, which were placed close to the patients' bones. The 50–800 mg/mL concentration provides a calibration for calculating the bone mineral density for the trabecular bone and 1000–1200 mg/mL concentration for the cortical bone.

Therefore, the resulting calibration equation was:

$$\rho = 0.01357 \bullet HU - 0.389 \tag{1}$$

2.2. Bone remodelling

The Stanford isotropic bone remodelling model (Jacobs, 1994) was developed with reference to the one presented by Beaupré et al. (1990). The model assumes that bone tissue has an isotropic, linear and elastic behaviour. In the present work, we used the following relationship between the bone mechanical properties and the density (Morgan et al., 2003), which has been validated based on experimental data (Schileo et al., 2007):

$$E = 6950\rho^{1.49} \tag{2}$$

where elastic modulus (E) is expressed in GPa, and density in g/cm^3.

Poisson's ratio has been assumed to be equal to 0.3 for the whole analysed bone.

The considered bone remodelling model takes into account that bone tissue is stimulated by a so-called daily tissue level stress stimulus, Ψ_t, defined as

$$\Psi_t = \left(\sum_{days} n_i \overline{\sigma}_{ti}^{m} \right)^{1/m}, \tag{3}$$

where n_i is the daily number of cycles of the load type I and $\overline{\sigma}_{ti}^{m}$ is the scalar that quantifies the effective stress in the region of bone tissue associated with the same load, and m is an empirical constant (Jacobs, 1994; Jacobs et al., 1997).

In essence, mechanical stimulus is a scalar governing the bone remodelling process and is dependent on the rate of remodelling $\dot{r}$. This rate indicates the possible changes in the material properties. In the described model, there are three criteria that determine the change in the properties. First of all, when the mechanical stimulus is greater than the reference value, bone apposition takes place. When the stimulus is smaller than the reference value, bone resorption occurs. Finally, when the stimulus is in a so-called 'dead zone', there is no change in the mechanical properties, and thus this stimulus is in a bone equilibrium state. The rate of remodelling can be described as

$$\dot{r} = \begin{cases} c[(\Psi_t - (\Psi_t^* - w)] & if\ \Psi_t < (\Psi_t^* - w), \\ 0 & if\ (\Psi_t^* - w) < \Psi_t < (\Psi_t^* + w), \\ c[(\Psi_t - (\Psi_t^* + w)] & if\ \Psi_t > (\Psi_t^* + w). \end{cases} \tag{4}$$

In this case, Ψ_t^* is the reference daily stress stimulus and defines a function when there is no change in the material properties (the so-called 'dead zone'), c is the slope of the bone remodelling curve, and w is the half-length of the dead zone.

For an apparent density ρ, the effective scalar stress can be related to the material continuum stress level called the apparent stress $\overline{\sigma}(\rho)$:

$$\overline{\sigma}(\rho) = \left(\frac{\rho}{\rho_c} \right)^2 \overline{\sigma}_t, \tag{5}$$

where ρ_c indicates the maximum value of the density for the cortical bone. The apparent stress is determined by

$$\overline{\sigma}_i(\rho) = \sqrt{2E(\rho)U_i(\rho)}, \tag{6}$$

where $E(\rho)$ is Young's modulus and $U_i(\rho)$ is the strain density energy, which is calculated as $U_i = U_i(\rho) = \frac{1}{2}\varepsilon_i : C(\rho) : \varepsilon_i$, where ε_i is the strain tensor and $C(\rho)$ is the elastic constants tensor.

The specific surface area, S_v, can be expressed in terms of the apparent density ρ (Corso, 2006). This parameter is a scalar that quantifies the internal surface of tissue in terms of its density and volume. The specific surface is obtained directly from a tomogram and can be written as

$$S_v = -0,07 + 8,1\rho - 7,2\rho^2 + 5,1\rho^3 - 2,1\rho^4 + 0,23\rho^5. \tag{7}$$

Finally, the rate of density evolution, $\dot{\rho}$, can be determined as

$$\dot{\rho} = S_v \dot{r} \rho_c. \tag{8}$$

The parameters that define the Stanford isotropic model (Jacobs, 1994) are presented in Table 1.

The finite element analysis is implemented using ABAQUS (version 6.14, Dassault Systems, 2015) software. The remodelling process is

Table 1
Values used for parameters in the simulation with the Stanford model.

Parameter	Value	Unity	Definition
Ψ^*	50	MPa	Reference stimulus
m	4	–	Exponent of the daily stress stimulus
c	0.02	μm/day	Remodelling velocity both for resorption and apposition
w	0.125* Ψ^*	MPa	Half-width of the dead zone
n	3000	–	Cycles per day
Δt	30	Days	Iteration time

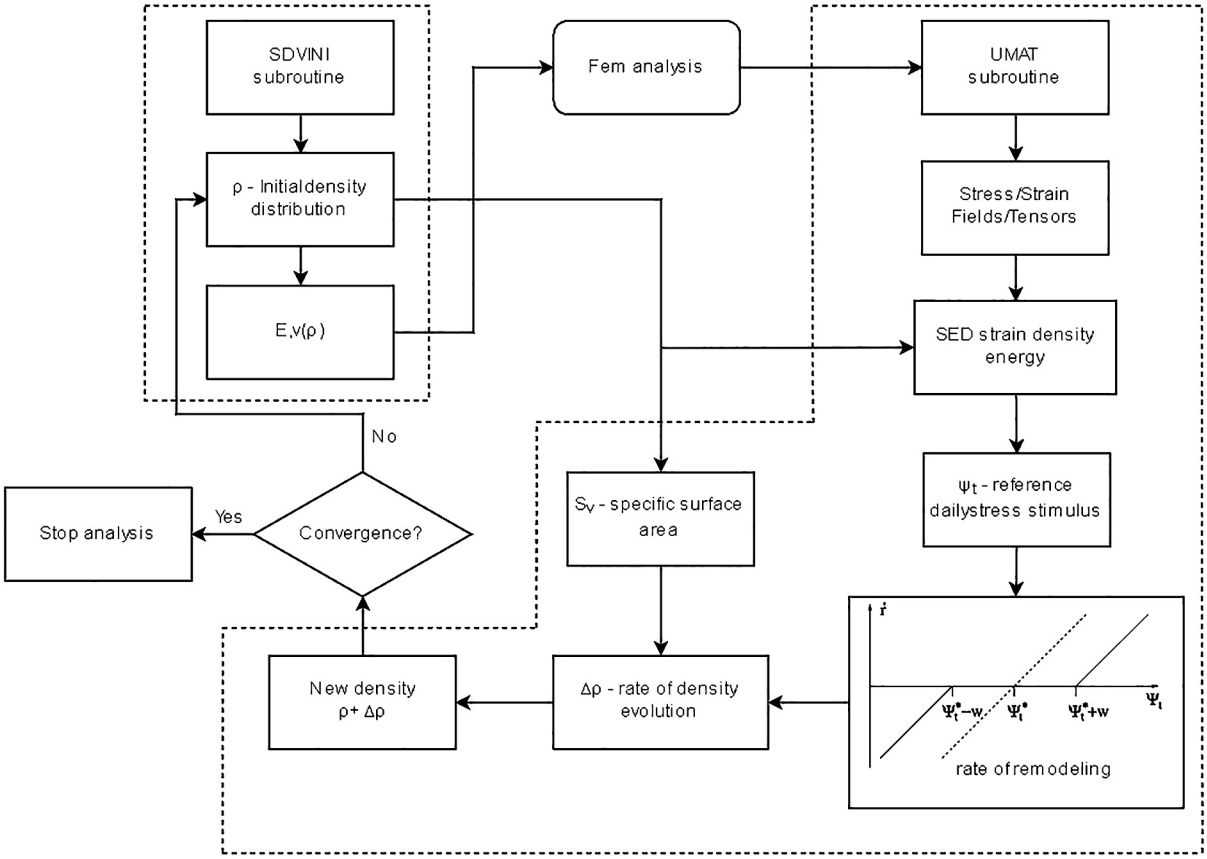

Fig. 2. A block diagram of the isotropic Stanford model algorithm.

divided into many time steps (Fig. 2). ABAQUS allows users to include custom subroutines, written in Fortran, to enhance the capabilities of analysis. In our work, a 'SDVINI' subroutine was used to import the initial density distribution obtained from CTs of the femur. Within each time step, the bone remodelling is embedded in the finite element analysis. In the element-based approach, the bone remodelling process is implemented through a user subroutine 'UMAT'. As illustrated in the bone remodelling algorithm (Fig. 2), for the next steps (iterations), new properties of each element are calculated based on the concentration of old and new bone remaining/produced inside the element. In this study, each remodelling period was chosen to denote one month. In total, 24 iterations were performed for every finite element model, simulating the remodelling period of two years.

2.3. Implant models

In this study, five of the most commonly used implant designs are presented (Fig. 3).

In the case of total hip replacements (THR), the femoral head is removed and replaced by a long, stemmed device (Fig. 3b and c). The procedure is reasonably successful in elderly, relatively inactive patients (McMinn et al., 2011). The main difference between tapered stems and stems with a square profile is the presence of an endoprosthesis collar (Fig. 3c) in the lower part of the neck, which rests on the cortical bone of the lesser trochanter (the arc of Adams). Short metaphyseal femoral stems have been developed in order to improve the results of standard cementless stems. The MAYO conservative hip system (Fig. 3e) and the PROXIMA hip system (Fig. 3d) were developed for the treatment of younger patients when the surgeon wants to conserve both the bone and the soft tissue and to provide physiological loading to the proximal femur. Hip resurfacing (HR) has been developed as a surgical alternative to THR. The HR procedure removes just a few millimetres of an articulating surface of the femur (Fig. 3f). The procedure is bone conserving, since most of the joint is retained. The femoral head is shaped in a way to accept a low-wear metal sphere. This sphere matches the patient's anatomy, assuring low risk of dislocation, a broad range of movement and excellent stability.

2.4. Boundary conditions

The interface between the bone and the implant is considered to be completely bonded, since relative micro-motions between the two parts must be prevented in real modular stems.

Contact load, acting from the acetabulum to the head of the endoprosthesis, can be represented as the principal vector F. Resultant force F can be represented as three components obtained in the decomposition of F on the axes of the local Cartesian coordinate system associated with the center of the head of the prosthesis (Fx, Fy, Fz). The value of these loads is calculated according to the experimental observations performed by Bergmann et al. (2001) on a patient who weighs 70 kg. In this case, the load acting on the femoral head was equal to: Fx = 520.1 N; Fy = 177.8 N; Fz = 1854.3 N.

In addition, in our study, only muscles that are predominant during the gait cycle were considered (i.e. hip abductors, tensor fasciae latae, vastus lateralis and vastus medialis). The applied loads correspond to the instant at 25% of the gait cycle that is a maximum loading of the femur during walking (Heller et al., 2005).

Titanium alloy (Ti6Al4V), having a Young's modulus E equal to 110,000 MPa and a Poisson's ratio of 0.3, was selected as the material of both femoral components of the hip endoprosthesis. Titanium alloys are generally preferred for orthopaedic applications due to their superior biocompatibility, high wear, corrosion resistance and reduced elastic modulus (Long and Rack, 1998).

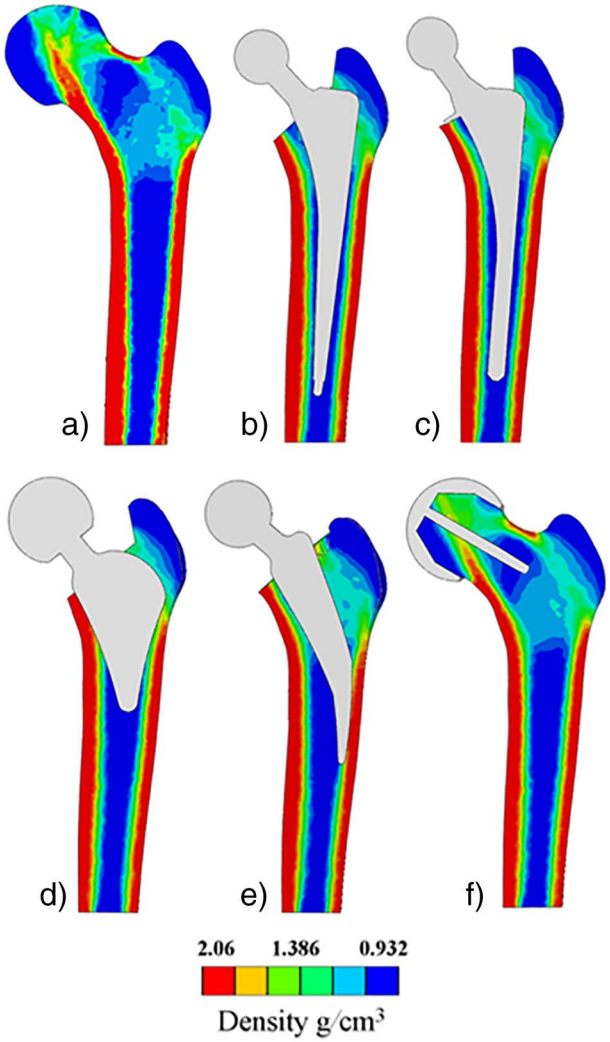

Fig. 3. Initial density distribution (a) before the THA and after the implementation of a (b) stem with collar, (c) tapered stem, (d) Mayo, (e) Proxima, and (f) resurfacing model.

3. Results

Using a 3D finite element model of a human femur, five different simulations were performed to investigate the effects of bone remodelling around different cementless femoral hip implants for each of the seven Gruen zones. The initial densities distribution is presented in Fig. 3a. Intact femur analysis provides mainly aspects of femoral morphology, such as the lateral and medial cortices, intermediary trabecular density distribution in the greater trochanter and femoral head, Ward's triangle in the femoral neck and the femoral canal in the diaphysis. This distribution is recovered and applied for each THA analysis; to do that, a set of routines is implemented in Matlab software. The recovery system attributes the elementary density value for the femur with stem models from the weighted average of all elements in a region in the intact femur mesh. The final distribution for each stem model analysis is shown in Fig. 4, where all changes are given in relation to intact bone. Bone remodelling simulations showed differences in final bone density distributions, which depend on the stem type.

Analysing the data obtained using the femoral component with a long-tapered stem (Fig. 4a) implanted in the femur canal, a decrease in the bone density in the proximal femur, in zones R1 R7 (by 15% (SD 4.8%) and 12% (SD 4%), respectively) was observed. Gruen zones 2 and 6 in the femoral diaphysis showed a low-level change in lateral and medial cortices ((6.8% (SD 2.2%) and 3% (SD 1%)) of changes approximately), what is not a meaningful change in relation to the initial condition. The Gruen zone, which is affected the most in the analysis, is number 4 in the distal part of the stem, which has 17% (SD 5.6%) of bone formation.

In the case of a long stem with a collar (Fig. 4b), the bone density after a 2-year post-operative period is distributed more evenly. The distribution of the bone density is similar to the case with a tapered stem, but the presence of the collar enables reduction of the change in the bone density in region R7 by approximately 4.7% (SD 1.1%). This corresponds to a low-level calcar resorption. The decrease in bone density was observed in the femoral diaphysis, in the same zones as in the tapered stem model. In zones R2 and R6, a meaningful difference in the change in the density before and after the surgery (about 5.3% (SD 1.2%) and 2.4% (SD 0.5%)) was not observed. There is a bone formation tendency, after two years of installation, for Gruen zones R3 and R4, due to the compression loads applied in the femoral head of the endoprosthesis.

The use of implants with a short stem enables the conservation of bone and soft tissue and provides an ability to transfer loads to the femur more evenly. In the case of the short-stem models, there are no significant differences in bone density between Mayo and Proxima stems. In Gruen zone R7, for both stems, there is a bone formation tendency (about 0.5–1%), and there is a low-level resorption for R1 (~1%). More load is transmitted to host bone in those cases. For other Gruen zones, there is no meaningful modification in density distribution. Utilisation of small components does not cause large modification in the femoral diaphysis.

The results have shown that in the case of using the resurfacing model (Fig. 4e), the bone density distribution in the post-operative period is closest to normal in comparison with other stems. Thanks to its design and geometry, the implant has an ability to more evenly transfer loads, similar to the case in healthy bone. In general, bone density change was insignificant (about 3–5%) in the whole bone.

Fig. 5 shows the percentage BMD change for seven Gruen zones. Based on this figure, it is possible to compare the influence of the prosthesis model on different regions of the bone–prosthesis interface. The bone density formation for long-stem components tends to have low-level load transmission in the proximal part. For small components, bone adaptation is softer for resorption (for Mayo and Proxima models), and variation in the bone density is smaller than in larger components. This means that the implant does not cause high-level adaptation at the interface with bone tissue. The last model (involving resurfacing) provides physiological loading to the femur, and density was insignificantly changed during the post-operative period.

In order to validate the FE results obtained in this study, we conducted radiometric studies of the bone with the help of highly trained and qualified orthopaedic surgeon with special interest in hip replacement. Analysing radiographs of patients with femoral components (the same as we used in our numerical study) two years after implantation (Fig. 6), the following results were obtained: in cases of tapered and collared implants, in zones R1 and R7, reduction in the density was observed. In zones R3, R4, R5, an increase in bone density was observed, which is typical for long-stem implants. For short-stem implants, significant reduction of bone density in zones R1 and R7 was not observed, while in the case of hip resurfacing, no significant difference in the values of the density in the short-term period and two years after surgery was noted. This comparison provides an overall qualitative assessment that the numerical models are ‘reasonable’.

For all considered fixation types of the prosthesis subjected to functional loads, intensity and distribution of stresses were obtained on both the medial and lateral sides of the stem and the femur. The applied loading conditions correspond to the peak hip contact forces during normal walking. In all cases of prosthesis application, the stress–strain state of the stem is determined by a combination of bending moments acting in the frontal plane and compression forces acting in the axial direction. Longitudinal tensile stress arises on the lateral side and the cervical part of the stem, while on the medial side, compressive stresses

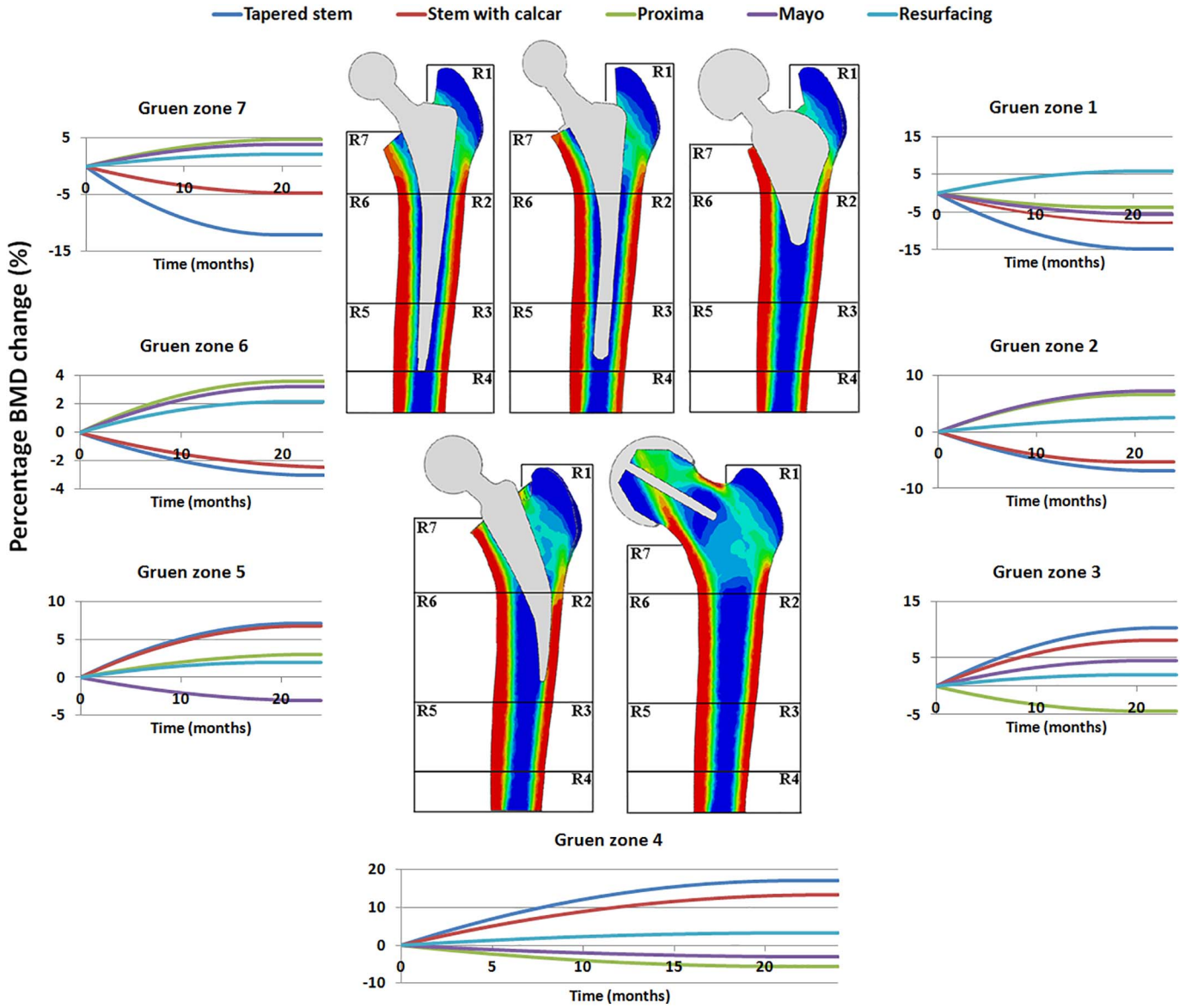

Fig. 4. Final density distribution for different models of endoprosthesis for 1st specimen, i.e. (a) tapered stem, (b) stem with collar, (c) Proxima, (d) Mayo and (e) Resurfacing model after a two-year analysis.

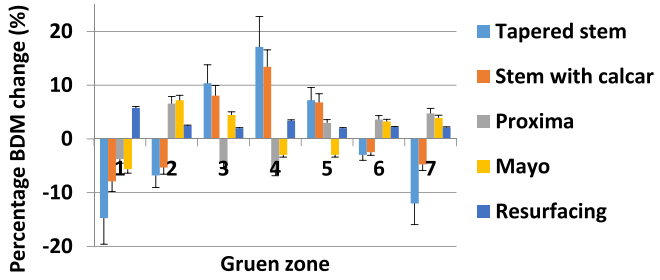

Fig. 5. Comparison of the change in BMD between different Gruen zones.

are present. The value of tensile stress in the endoprosthesis is less than of the compressive stress. For all types of implants, the results have shown that the maximum stresses in the elements of the assembly have not exceeded the yield strength of the material, and all elements of the system were in a state of elastic deformation. Distribution of stress in the femur is similar to the bone density distribution. On the lateral side of the femur, normal tensile longitudinal stress is present, while on the medial side, compressive stresses arise. Comparison of maximum tensile and compressive stresses in the femoral bone has shown that stress values on lateral and medial sides differ on average by 15%. This is important, since mechanical properties of bone in tension are 1.5 times worse than those of bone in compression.

4. Discussion

This paper aims at evaluation and verification of the bone remodelling process before and after implantation of different models of a femoral prosthesis. Through the density distributions after two years of the installation of different cementless femoral hip implants, we can note that the geometry of the model is the fundamental factor for the success of treatment.

When the obtained numerical results are qualitatively compared with clinical ones, similarities in density distributions can be noted. The effect caused by implantation of a component more rigid than bone tissue results in bone adaptation to the new mode of load application, which has been confirmed by numerical results following the clinical ones (Boschin and Alencar, 2007; McLaughlin and Lee, 1997; McLaughlin and Lee, 2014; Wittenberg and Steffen, 2015). Another

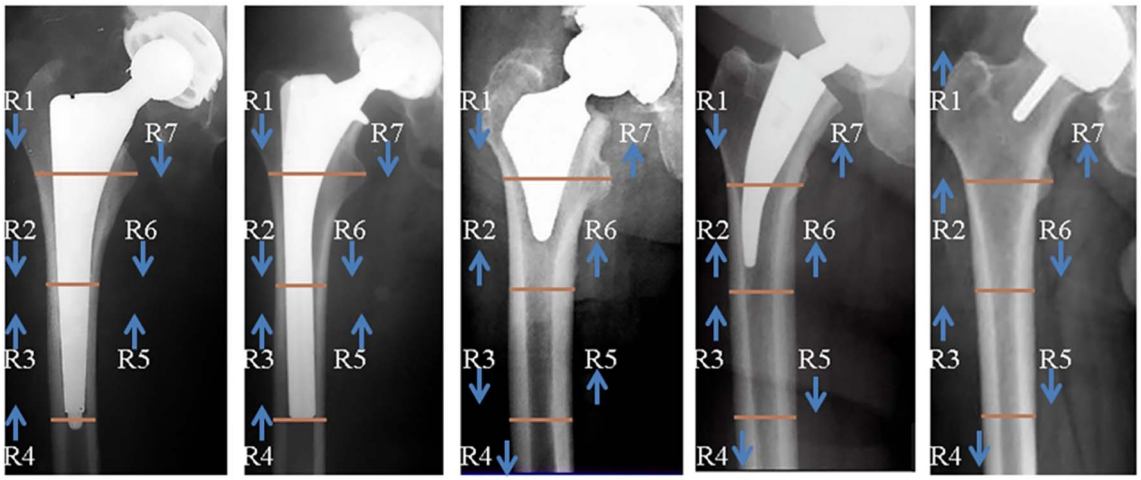

Fig. 6. Radiographs of the prosthetic limb two years after implantation: an up arrow shows an increase in bone density, while a down arrow indicates a decrease.

similar effect noted from numerical results is the largest variation in the bone density distribution that takes place until the end of the first year after THA and becomes practically constant during the rest of the analysis, as found by other authors (Gibbons et al., 2001; Huiskes et al., 1989; Panisello et al., 2009; Sköldenberg et al., 2006; Sychter and Engh, 1996). It should be noted, however, that there are also other studies that have found variation in the density until the end of the second year after the THA (Herrera et al., 2008; Scanell and Prendergast, 2009; Kwon et al., 2013; Herrera et al., 2014; Jake and Scott, 1996; Nysted et al., 2011).

Significant differences in bone mineral density were identified in the femur in comparing the long stem, short stem, and resurfacing implants. These differences arise because of changes in the load transfer patterns between the implants and bone. In the intact bone, the load is transmitted to the femoral head, then to the medial cortical bone of the femoral neck towards the lesser trochanter, where they are distributed by the diaphyseal bone. However, in the reconstructed femurs, with the long stem the load is applied to the implant, which is then transferred to the distal bone through a stem, instead of diffusely into the central and proximal part of the bone. Therefore, stress shielding, whereby bone is subjected to less stress than in the intact model, is experienced in the proximal sections of the cortical shell and cortical hypertrophy in the distal part (Sköldenberg et al., 2006), whereby an increase in the density and volume of the bone tissue are observed because of altered load transfer pathways. Our results have confirmed this: in the case of a tapered stem being used, there are significant increases in the distal part (Gruen zone 4 by 17% (SD 5.6%)) and a decrease in the proximal part - (Gruen zone 1 by 15% (SD 4.8%)).

Femoral components of hip prostheses are also available with collars. From the viewpoint of engineering design, a collar is designed to transmit axial loads to the bone of the divided neck on which it rests. Such a design can provide more even loading in the same manner as in a natural femur, and minimize bone loss from stress shielding of the proximal part. The collar also helps to ensure axial stability of the prosthesis. Our results have shown that in the case of a collar stem being used, decreasing of cortical hypertrophy in the distal part (Gruen zone 4 by 17% (SD 5.6%)) and stress shielding of the proximal part of the femur (Gruen zone 1 by 17% (SD 5.6%)) are observed in comparison to collarless long stems.

A significant decrease in proximal bone stress shielding and distal hypertrophy were identified with the short stem models (Gruen zone 1 by 15% (SD 4.8%) and Gruen zone 4 by 17% (SD 5.6%)). Because short stem models have no mechanism for distal load transfer, all of the joint reaction force is transferred across a shorter interface, resulting in significant changes in bone density in proximal and distal parts relative to long stem implant models (Santori and Santori, 2010; Stulberg and Patel, 2013).

Hip resurfacing is an alternative form of hip arthroplasty that conserves proximal femoral bone and provides good hip stability. However, for fixation requirements head and neck of femur. Failure of hip resurfacing can be associated with fracture of the femoral neck in the short term and aseptic loosening due to bone resorption of the femoral head in the long term (Laffosse et al., 2011; Lilikakis et al., 2005). However, our results have shown that during postoperative 2-year analysis, bone mineral density in the femoral neck (and in other Gruen zones) after resurfacing remained equal or even increased slightly. Due to its design and geometry, the implant can transfer loads more evenly, such as is the case for healthy bone, and bone density distribution in the post-operative period is closest to normal (Gruen zone 1 by 5.7% (SD 0.2%) and Gruen zone 4 by 3.3% (SD 0.16%)).

While comparing numerical and clinical results, it is worth mentioning that behaviour of a prosthesis strongly depends on the human organism. As can be seen in clinical research (Boschin and Alencar, 2007; McLaughlin and Lee, 1997; McLaughlin and Lee, 2014), the same prosthesis model can produce different distributions at the same time. Bone adaptation around the prosthesis differs in each individual. Employment of an implant modifies the density distribution and the stress field. Thus, bone tissue is stimulated in a different way than before THA, which evidences Wolff's law, according to which bone tissue adapts itself to the loads to which it is subjected.

Although the clinical and numerical results can be qualitatively compared, the analysis of the bone remodelling process around the prosthesis assumes some simplifications. First, the bone–prosthesis interface is considered with complete bone adhesion. Such a condition is unreal, due to the possibility of the occurrence of non-uniformity of load transfer over the interface, which can, in turn, generate bone resorption points. Second, the bone remodelling model does not consider the osseointegration process occurring at the interface, which is very important while simulating an interface without cement. Third, the load condition, simulating walking and other aspects, is not applied in the model. Nevertheless, even with all those simplifications, the FEM simulation provides a bone density distribution that enables a qualitative comparison with clinical results, which shows the importance of this method in solving several engineering problems.

5. Conclusions

The paper presents the results of application of the numerical analysis, which allowed determination of the relationship between two-year bone adaptation to mechanical loading and different endoprosthesis types. In order to obtain reliable results of the finite element analysis, model generation of both femur and prostheses of real size and

shape, as well as the physico–mechanical properties of the material and the values of the functional load have been employed while carrying out the modelling process and numerical simulations. Clinical results of the use of the described prostheses in hip replacement surgery confirm the results obtained with the numerical approach and enable implementation of the isotropic Stanford model in the analysis of bone remodelling around the femoral prosthesis. Evidently, it is hard to say which stem is better, because the use of different types of fixation depends on many factors such as the weight of the patient, the bone condition, osteoporosis, lifestyle and age. However, the results of this study suggest that the use of a prosthesis with a collar could substantially reduce proximal stress shielding of the femur in comparison with a collarless stem, while the use of a short stem prosthesis transfers load even more evenly to the proximal and distal femur. Finally, the results have shown that in the case of hip resurfacing, bone mineral density during the postoperative 2-year period changes slightly and is closest to intact femur.

Acknowledgment

This work was supported by the National Science Center of Poland under the grant OPUS 9 No. 2015/17/B/ST8/01700 for years 2016–2018.

Conflict of interest statement

The authors have no conflict of interest.

References

Beaupré, G.S., Orr, T.E., Carter, D.R., 1990. An approach for time-dependent bone modelling and remodelling-application: a preliminary remodeling simulation. J. Orthop. Res. 8 (5), 651–661. http://dx.doi.org/10.1002/jor.1100080507.

Bergmann, G., Deuretzbacher, G., Heller, M., Graichen, F., Rohlmann, A., Strauss, J., Duda, G.N., 2001. Hip contact forces and gait patterns from routine activities. J. Biomech. 34 (7), 859–871.

Boschin, L.C., Alencar, P.G.C., 2007. Stress shielding: radiographic evaluation after long term follow-up. Rev. Bras. Ortop. 42 (9), 290–296.

Cann, C., 1988. Quantitative CT for determination of bone mineral density: a review. J. Radiol. 166 (1), 509–522. http://dx.doi.org/10.1148/radiology.166.2.3275985.

Corso, L.L., 2006. Application of Optimization Procedures and Bone Remodeling in a Simulation and Analysis of Biomechanics Problems, MSc (Degree thesis). Federal University of Rio, Grande do Sul.

De Santis, R., Ambrosio, L., Nicolais, L., 2000. Polymer–based composite hip prostheses. J. Inorg. Biochem. 79 (1–4), 97–102.

Engh Jr, C.A., Sychterz, C., Engh Sr, C., 1999. Factors affecting femoral bone remodeling after cementless total hip arthroplasty. J. Arthroplast. 14 (5), 637–644.

Ethgen, O., Bruyère, O., Richy, F., Dardennes, C., Reginster, J.Y., 2004. Health–related quality of life in total hip and total knee arthroplasty. A qualitative and systematic review of the literature. J. Bone Joint Surg. Am. 86–A (5), 963–974.

Froimson, M.I., Garino, J., Machenaud, A., Vidalain, J.P., 2007. Minimum 10–year results of a tapered, titanium, hydroxyapatite–coated hip stem: an independent review. J. Arthroplast. 22 (1), 1–7. http://dx.doi.org/10.1016/j.arth.2006.03.003.

Gibbons, C., Davis, A., Amis, A.A., Scott, J.E., 2001. Periprosthetic bone mineral density changes with femoral components of different design philosophy. Int. Orthop. 25 (2), 89–92. http://dx.doi.org/10.1007/s002640100246.

Heller, M.O., Bergmann, G., Kassi, J.-P., Claes, L., Haas, N.P., Duda, G.N., 2005. Determination of muscle loading at the hip joint for use in pre-clinical testing. J. Biomech. 38 (5), 1155–1163. http://dx.doi.org/10.1016/j.jbiomech.2004.05.022.

Herrera, A., Panisello, J.J., Ibarz, E., Cegoñino, J.A., Gracia, L., 2008. Densitometric and finite-element analysis of bone remodeling further to implantation of an uncemented anatomical femoral stem. Revista de Cirurgía Ortopédica y trumatológica 52 (5), 269–282.

Herrera, A., Rebollo, S., Ibalz, E., Mateo, J., Gabarre, S., Gracia, L., 2014. Mid-term study of boné remodelling after femoral cemented stem implantation: comparison between DXA and finite element simulation. J. Arthroplast. 29 (1), 90–100. http://dx.doi.org/10.1016/j.arth.2013.03.028.

Huiskes, R., Weinans, H., Dalstra, M., 1989. Adaptative bone remodeling and biomechanical design considerations for noncemented total hip arthroplasty. Orthopaedics 12 (9), 1255–1267.

Jacobs, C.R., 1994. Numerical Simulation of Bone Adaptation to Mechanical Loading (PhD thesis). Stanford University.

Jacobs, C.R., Simo, J.C., Beaupré, G.S., Carter, D.R., 1997. Adaptive bone remodeling incorporating simultaneous density and anisotropy considerations. J. Biomech. 30 (6), 603–613.

Jake, W.L., Scott, D.F., 1996. Current concepts and review. Total hip arthroplasty with hydroxyapatite-coated prostheses. J. Bone Joint Surg. 78 (12), 1918–1934.

Jenkins, P.J., Clement, N.D., Hamilton, D.F., Gaston, P., Patton, J.T., Howie, C.R., 2013. Predicting the cost–effectiveness of total hip and knee replacement: a health economic analysis. J.Bone Joint 95–B (1), 115–121. http://dx.doi.org/10.1302/0301-620X.95B1.29835.

Kelly, M.A., Dalury, D.F., Kim, R.H., Backstein, D., 2009. The new arthritic patient and nonarthroplasty treatment options. J. Bone Joint Surg. Am. 91 (5), 40–42. http://dx.doi.org/10.2106/JBJS.I.00367.

Kwon, J.Y., Naito, H., Matsumoto, T., Tanaka, M., 2013. Estimation of change of bone structures after total hip replacement using bone remodeling simulation. Clin. Biomech. 28 (5), 514–518.

Laffosse, J.M., Aubin, K., Lavigne, M., Roy, A., Vendittoli, P.A., 2011. Radiographic changes of the femoral neck after total hip resurfacing. Orthop.Traumatol. Surg. Res. 97 (3), 229–240. http://dx.doi.org/10.1016/j.otsr.2011.01.011.

Lemaire, V., Tobin, F.L., Greller, L.D., Cho, C.R., Suva, L.J., 2004. Modeling the interactions between osteoblast and osteoclast activities in bone remodeling. J. Theor. Biol. 229 (3), 293–309. http://dx.doi.org/10.1016/j.jtbi.2004.03.023.

Lilikakis, A.K., Vowler, S.L., Villar, R.N., 2005. Hydroxyapatite-coated femoral implant in metal-on-metal resurfacing hip arthroplasty: minimum of two ears follow-up. Orthop. Clin. N. Am. 36 (2), 215–222. http://dx.doi.org/10.1016/j.ocl.2004.12.003.

Long, M., Rack, H.J., 1998. Titanium alloys in total joint replacement – a materials science perspective. Biomaterials 19 (18), 1621–1639.

McLaughlin, J.R., Lee, K.R., 1997. Total hip arthroplasty with an uncemented femoral component. Excellent results at ten-year follow-up. J. Bone Joint Surg. 79, 900–907.

McLaughlin, J.R., Lee, K.R., 2014. Uncemented total hip arthroplasty using a tapered femoral component in obese patients: an 18–27 year follow-up study. J. Arthroplast. 29 (7), 1365–1368. http://dx.doi.org/10.1016/j.arth.2014.02.019.

McMinn, D.J., Daniel, J., Ziaee, H., Pradhan, C., 2011. Indications and results of hip resurfacing. J. Int. Orthop. 35 (2), 231–237. http://dx.doi.org/10.1007/s00264-010-1148-8.

Morgan, E.F., Bayraktar, H.H., Keaveny, T.M., 2003. Trabecular bone modulus-density relationships depend on anatomic site. J. Biomech. 36 (7), 897–904.

Nysted, M., Benum, P., Klaksvik, J., Foss, O., Aamodt, A., 2011. Periprosthetic bone loss after insertion of an uncemented, customized femoral stem and an uncemented anatomical stem. Acta Orthop. 82 (4), 410–416. http://dx.doi.org/10.3109/17453674.2011.588860.

Pal, B., Gupta, S., New, A.M.R., 2010. Influence of the change in stem length on the load transfer and bone remodeling for a cemented resurfaced femur. J. Biomech. 43 (15), 2908–2914. http://dx.doi.org/10.1016/j.jbiomech.2010.07.017.

Panisello, J.J., Herrero, L., Canales, V., Herrera, A., Martinez, A.A., Mateo, J., 2009. Long-term remodeling in proximal femur around a hydroxyapatite-coated anatomic stem: ten years densitometric follow up. J. Arthroplast. 24 (1), 56–64. http://dx.doi.org/10.1016/j.arth.2007.12.017.

Peng, L., Bai, J., Zeng, X., Zhou, Y., 2007. Comparison of isotropic and orthotropic material property assignments on femoral finite element models under two loading conditions. J. Med. Eng. Phys. 28 (3), 227–233. http://dx.doi.org/10.1016/j.medengphy.2005.06.003.

Rothstock, S., Uhlenbrock, A., Bishop, N., Laird, L., Nassutt, R., Morlock, M., 2011. Influence on interface condition and implant design on bone remodeling and failure risk for the resurfaced femoral head. J. Biomech. 44 (9), 1646–1653. http://dx.doi.org/10.1016/j.jbiomech.2011.02.076.

Sabatini, A.L., Goswami, T., 2008. Hip implants VII: finite element analysis and optimization of cross–sections. J. Mater. Des. 29 (1), 1438–1446. http://dx.doi.org/10.1016/j.matdes.2007.09.002.

Santori, F.S., Santori, N., 2010. Mid-term results of a custom-made short proximal loading femoral component. J. Bone Joint Surg. 92 (9), 1231–1237. http://dx.doi.org/10.1302/0301-620X.92B9.24605.

Scanell, P.T., Prendergast, P.J., 2009. Cortical and interfacial bone changes around a non-cemented hip implant: simulations using a combined strain/damaged remodeling algorithm. Med. Eng. Phys. 31 (4), 477–488. http://dx.doi.org/10.1016/j.medengphy.2008.11.007.

Schileo, E., Taddei, F., Malandrino, A., Cristofolini, L., Viceconti, M., 2007. Subject-specific finite element models can accurately predict strain levels in long bones. J. Biomech. 40 (13), 2982–2989. http://dx.doi.org/10.1016/j.jbiomech.2007.02.010.

Senalp, A.Z., Kayabasi, O., Kurtaram, H., 2007. Static, dynamic and fatigue behavior of newly designed stem shapes for hip prosthesis using finite element analysis. Mater. Des. 28 (5), 1577–1583. http://dx.doi.org/10.1016/j.matdes.2006.02.015.

Sköldenberg, O.G., Bodén, H.S.G., Salemyr, M.O.F., Ahl, T.E., Adolphson, P.Y., 2006. Periprosthetic proximal bone loss after uncemented hip arthroplasty is related to stem size: DXA measurements in 138 patients followed for 2–7 years. Acta Orthop. 77 (3), 386–392. http://dx.doi.org/10.1080/17453670610046307.

Stulberg, S.D., Patel, R.M., 2013. The short stem. Promises and pitfalls. Bone Joint J. 95-B (11 Suppl. A), 57–62. http://dx.doi.org/10.1302/0301-620X.95B11.32936.

Sumner, D.R., 2015. Long–term implant fixation and stress–shielding in total hip replacement. J. Biomech. 48 (5), 797–800. http://dx.doi.org/10.1016/j.jbiomech.2014.12.021.

Sychter, C.J., Engh, C.A., 1996. The influence of clinical factor on periprosthetic bone remodeling. Clin. Orthop. Relat. Res. 322, 285–292.

Wittenberg, R.H., Steffen, R., 2015. Comparative 5-year results of short hip total hip arthroplasty with Ti- or CoCr-Neck Adapters. Orthopedics 38 (3), S33–S39. http://dx.doi.org/10.3928/01477447-20150215-54.

Yamako, G., Chosa, E., Zhao, X., Totoribe, K., Watanabe, S., Sakamoto, T., Nakane, N., 2014. Load–transfer analysis after insertion of cementless anatomical femoral stem using pre– and post–operative CT images based patient–specific finite element analysis. J. Med. Eng. Phys. 36 (6), 694–700. http://dx.doi.org/10.1016/j.medengphy.2014.02.018.